Neuroendocrinology Letters Vol. 35 No. 6 2014
ISSN: 0172-780X; ISSN-L: 0172-780X; Electronic/Online ISSN: 2354-4716
Web of Knowledge / Web of Science: Neuroendocrinol Lett
Pub Med / Medline: Neuro Endocrinol Lett

Dot1L mediated histone H3 lysine79 methylation is essential to meiosis progression in mouse oocytes

Xuguang Wang [1,2,#], Wenlong Gao [1,#], Xueshan Ma [1], Xiaona Wang [1], Chunlei Song [1], Xianju Huang [1], Honglin Liu [1]

1 College of Animal Science and Technology, Nanjing Agricultural University, Nanjing, China
2 College of Animal Science, Xinjiang Agricultural University, Urumqi, China

[#] *Both authors contributed equally to this work*

Correspondence to: Honglin Liu
College of Animal Science and Technology,
Nanjing Agricultural University,
No.1 Weigang Nanjing, 210095, China.
TEL: +86-025-84395106; FAX: +86-025-84395314; E-MAIL: liuhonglin@njau.edu.cn

Submitted: 2014-10-16 Accepted: 2014-10-18 Published online: 2014-11-29

Key words: ***Dot1l*; RNA interference; H3K79 methylation; mouse oocyte; meiosis; Dot1L protein**

Neuroendocrinol Lett 2014; **35**(6):523–530 **PMID:** 25433842 NEL350614A14

Abstract

OBJECTIVES: Post-translational modifications of lysine residues of histones can result in a series of functional changes. Lysine 79 of histone H3 (H3K79) can be methylated specifically by the Dot1 family of histone lysine methyltransferases. Although multiple developmental abnormalities in Dot1L-deficient mouse embryos have been studied, the biological function of H3K79 methylation in mammal oocytes remains unclear. Here, the distribution of Dot1L, methyltransferase of residue lys79 of histone H3 (H3K79) in mouse, and its effect on mouse oocytes meiosis were investigated to examine whether there are changes in the pattern of distribution and effect of Dot1L on mouse oocytes meiosis.

METHODS: The mRNA level of Dot1l in mouse oocytes was examined using real-time qPCR (RT-qPCR) technique. The distribution and level of Dot1L protein and H3K79 methylation were examined using immunofluorescence and western-blot techniques, respectively. The down regulation of Dot1l in mouse oocytes was conducted using siRNA injection technique.

RESULTS: Dot1L was detected diffuse staining in the nuclear of mouse GV (Germinal Vesicle) stage oocytes. The Dot1l expression and H3K79 methylation level were suppressed effectively with anti-Dot1l siRNA injection. In Dot1L deficient, accompanying with BubR1 (MAD3/Bub1b) remains on the chromosome, the mouse oocytes was blocked in metaphase of meiosis I. The histone deacetylation was also incomplete in Dot1L-deficient mouse oocytes.

CONCLUSION: Dot1L protein is well distributed in mouse GV stage oocytes. Dot1L and H3K79 methylation play important roles in meiosis progression and are supposed to be associated with chromosome deacetylation of mouse oocytes.
.

ORIGINAL ARTICLE

Abbreviations:

DOT1	- Disrupter of telomere silencing protein 1, Lysine N-methyltransferase 4 [*Saccharomyces cerevisiae*]
DOT1L	- DOT1 like protein [*Homo sapiens*]
Dot1L	- DOT1 like protein [*Mus musculus*]
H3K79	- Histone 3 lysine-79
H3K79me1(2,3)	- H3K79 mono-(di-,tri-)methylation
H3K27ac	- Histone 3 lysine-27 acetylation
H4K12ac	- Histone 4 lysine-12 acetylation
IVM	- *in vitro* mature
PMSG	- pregnant mare's serum gonadotrophin
GV	- Germinal vesicle
GVBD	- Germinal vesicle break down
IBMX	- 3-Isobutyl-1-methylxanthine
PVP	- Polyvinylpyrrolidone

INTRODUCTION

The nucleosome contains 146bp of DNA wrapped around a histone protein octamer composed of two copies of each histone protein (H2A, H2B, H3 and H4). The N-terminal tail of histones can undergo post-translational modifications such as methylation, acetylation, ubiquitination, and ADP ribosylation (Kouzarides 2007; Li *et al.* 2007). Histones can be methylated on lysine residues and arginine residues. Histone lysines have been found mono-, di-, or tri-methylated on residues lys4, 9, 27, 36 and 79 of histone H3 and Lys20 of histone H4. The *dot1* gene of *Saccharomyces cerevisiae* was initially isolated in a genetic screen for high-copy disruptors of telomere (DOT) silencing. Telomere silencing was subsequently shown to be reduced by *dot1* deletion (Singer *et al.* 1998). DOT1 can catalyze the mono- (me1), di-(me2) and tri-methylation (me3) of H3K79 in yeast (Feng *et al.* 2002), which occurs within the core domain of histone H3. The DOT1 and its homologues in other species (DOT1L in human and Dot1L in mouse) are the few known H3K79 methyltransferases. Methylation of H3K79 is highly conserved from yeast to mammals (Feng *et al.* 2002; Kim *et al.* 2012a). Most of the histone methyltransferases characterized to date contain a SET domain, named after D. melanogaster Su(var)3-9, Enhancer of zeste (E(z)), and Trithorax (trx). However, DOT1 is different as it lacks a SET domain and modifies nucleosomal histones rather than free histones (Feng *et al.* 2002). Histone lysine methylation is also reversible. KDM1 and JMJC families of histone demethylase have been characterized (Braunstein *et al.* 1993), but the demethylase for H3K79 is still unclear. For the function of H3K79 methylation, H3K79me1 and me2 are modestly associated with active transcription (Barski *et al.* 2007). H3K79me3 is correlative with neither active genes nor silent genes in yeast (Pokholok *et al.* 2005), instead, it is associated with gene repression in human cells (Barski *et al.* 2007). It has been suggested that H3K79me2 is related to checkpoint in G1/S progression in cell cycle and DNA double strand break repair (Oksenych *et al.* 2013), while H3K79me3 is a marker for heterochromatin (Ooga *et al.* 2008).

Previous studies have shown that DOT1 (or its homologues)-mediated histone H3K79 methylation played an important role in regulation of chromatin dynamics and gene activity from fungi to mammals (Jones *et al.* 2008; Kim *et al.* 2012b). The distribution of H3K79 methylation in mouse oocyte and preimplantation embryos has also been reported (Ooga *et al.* 2008). Nevertheless, the role of histone H3K79 methylation in meiosis in mammals is still unclear. In the present study, we analyzed the distribution pattern of Dot1L and histone H3K79 methylation in mouse oocytes. The expression of Dot1L and the level of histone H3K79 methylation were down-regulated, by using RNA interference (RNAi), a widely used technology that provides rapid suppression of specific genes (Wianny & Zernicka-Goetz 2000; Yu *et al.* 2004). The results demonstrated that Dot1L mediated H3K79 methylation plays important role in mouse oocytes meiotic progression.

MATERIALS AND METHODS

All culture media and chemicals were purchased from Sigma-Aldrich (St. Louis, MO, USA) and all antibodies were purchased from Abcam Trading (Shanghai) Company Ltd. (Shanghai, China) unless stated otherwise.

siRNA design and synthesis

The chemical synthetic 25nt siRNA were obtained from Invitrogen Stealth™ RNAi product. The sequences of siRNA for *Dot1l* (gene ID: 208266) were designed using the Invitrogen program BLOCK-iT RNAi Designer. The siRNA (UUUCCAUACCAUUUCAUC CACUUCC) targeting sequence for *Dot1l* mRNA (NM_199322.1) matched 608–632nts. The siRNA (UUUCUCCAUACCAUUUCAUCCAUCC) that possess the scrambled sequence of cognate siRNA was used as negative control.

Mouse oocytes collection, microinjection, and culture

Three-week-old female ICR mice (Qinglongshan Experimental Animal Center, Nanjing, China) were superovulated with 10 IU of pregnant mare's serum gonadotrophin (PMSG) (Ningbo Second Hormone Factory, Zhejiang China). 47h later, Germinal vesicle (GV) oocyte were isolated by rupturing of antral ovarian follicles in M2 medium, supplemented with 3 mg/ml of Bovine Serum Albumin (BSA) and 0.2 mmol/l of 3-Isobutyl-1-methylxanthine (IBMX). The cumulus cells surrounding the oocyte were removed by gentle pipetting, and the GV oocytes were collected. The oocytes were washed 3 times in M2 medium with IBMX and divided into 3 groups randomly for *Dot1l* siRNA microinjection, scrambled RNA microinjection and no injection. After microinjection, the survived oocytes and the oocytes in control group were transferred respectively into IVM (*in vitro* mature) medium with IMBX, α-MEM medium (Gibco, Life Technologies, Shanghai, China) supplemented with 5% fetal bovine serum (FBS, Gibco, Life Technologies,

Shanghai, China), 10μg /ml of epidermal growth factor (EGF) and 0.2 mmol/l of IBMX, incubated for 24 h in an incubator of saturated humidity, atmosphere of 5% CO_2/95% air at 37 °C. And then oocytes subjected to RNA extraction, immunocytochemistry or transferred to fresh IVM medium, α-MEM medium with 5% FBS, 10 μg/ml of EGF, and incubated for 12h to check the performance of meiotic maturation. Care and handing of mice were conducted in accordance with policies promulgated by the Ethics Committee of the Institute of Zoology, Chinese Academy of Sciences.

Oocytes were microinjected in M2 medium supplemented with IBMX. Microinjection was performed on the inverted microscopes (IX71, OLYMPUS) with IM-300(NARISHGE) micromanipulator. About 10 pl of 1 μg/μl siRNA duplexes were injected into the cytoplasm of each GV oocyte.

RNA isolation and real-time qPCR analyses

Total RNA was isolated from about 80 oocytes with 400 μl TRIzol reagent (Invitrogen, Life Technologies, Inc, California, USA) following the instruction. RNA samples isolated from oocytes were reverse-transcribed in a 25 μl reaction mixture that contained 200 U M-MLV Reverse Transcriptase (Shanghai Promega Biological Products, Ltd. Shanghai, China) and 0.5 μg oligo (dT) 15 primer (Invitrogen, Life Technologies, Inc, California, USA).

The synthesized cDNA served as the template. Real-time qPCR was performed as previously described (Hara *et al.* 2003). RT-qPCR amplification with SYBR Green Pre-mix (Takara Biotechnology (Dalian) Co. Ltd., Dalian China) was performed for 40 cycles on an ABI Prism 7300. The relative amount of each sample was determined based on a standard curve obtained by amplifying a 10-fold dilution series of purified PCR product of *Dot1l*. Gene *β-actin* was used for normalization. The following primers were used: mouse *Dot1l* (forward) 5'-TGGTCCTGAGGTGGATCACCAG-3' and (reverse) 5'-AGTTTTCAAGTATGGTGCGGTC-3'; mouse *β-actin* (forward) 5'-GCTGTCCCTGTATGCCTCT-3' and (reverse) 5'-GTCTTTACGGATGTCAACG-3'.

Immunofluorescence

The oocytes were immunostained as described previously with slight modification (Liu *et al.* 2004). In brief, the oocytes were fixed with 3.7% paraformaldehyde in PBS overnight at 4 °C and permeabilized with 0.5% Triton X-100 for 15 min. Then the oocytes were incubated with the primary antibodies overnight at 4 °C. The antibodies that bound to the oocyte were probed with Alex 488 anti-rabbit IgG (Invitrogen, Life Technologies, Inc, California, USA) or Alex 594 anti-rabbit IgG (Invitrogen, Life Technologies, Inc, California, USA), Alex 488 anti-mouse IgG (Invitrogen, Life Technologies, Inc, California, USA), FITC anti-sheep IgG for 1h at room temperature, respectively. Counterstaining was conducted with DAPI. Fluorescence was detected by a Carl Zeiss LSM700 laser scanning confocal microscope and exposure time for each section were kept constant in the same experiment. The primary antibodies were anti-H3K79me2 (ab3594, 1:200), anti-H3K79me3 (ab2621, 1:100), anti-Dot1L (ab64077, 1:100), anti-BubR1 (ab28194, 1:100), anti-H3K27ac (ab4729, 1:200) and anti-H4K12ac (ab46983, 1:200), respectively.

Semi-quantitative analysis of the fluorescence signals was conducted using the NIH Image program (National Institute of Health, Bethesda, MD, USA), as described previously (Ontoso *et al.* 2013). At least three independent experiments containing at least 20 oocytes of each treatment were conducted.

Protein isolation and Western-blot analyses

The Western-blot analysis of oocytes was performed as previously described (Peters *et al.* 2001) with some modifications. Briefly, 300 oocytes per treatment were pooled at 24 h after injection, washed in PBS medium containing 0.1% Polyvinylpyrrolidone (PVP) and directly pipetted into 15 μl of 5× SDS loading buffer. Samples were denatured for 3 minutes at 95 °C. Proteins were separated on a 7.5% SDS gel and blotted onto pure nitrocellulose blotting membranes (Biotrace, pall life science). The membrane was blocked in TBST (150 mM NaCl, 50 mM Tris/HCl [pH 7.5], and 0.1% Tween 20) containing 3% BSA for 2 hours. After incubation with anti-Dot1L or anti-α-tubulin antibody (clone B-5-1-2, Sigma-Aldrich Shanghai, China) overnight at 4 °C, rinsing in TBST several times, the bound IgG were detected with HRP conjugated goat anti-rabbit IgG (ICL, Inc., Portland, OR, USA) or goat anti-mouse IgG (ICL, Inc., Portland, OR, USA) followed by ECL detection (Premier, Thermo Fisher Scientific Inc., Waltham, MA, USA).

Statistical analysis

One-way ANOVA was used to evaluate the difference between treatments in RT-qPCR or immunofluorescence (IF) staining qualified data. Data was presented as the mean of at least three independent experiments; variation among replicates was presented as the mean, standard deviation (s.d.). X^2 test was used to evaluate the ratio of germinal vesicle break down (GVBD %) and extrusion ratio of the first polar body (PB1%).

RESULTS

Subnuclear localization of Dot1L in oocytes

The pattern of subnuclear localization of Dot1L, and H3K79 di-, tri-methylation was investigated firstly. Immunofluorescence results showed that Dot1L was detected in the nuclear of GV stage oocytes (Figure 1A, No Injection treatment), and surrounding the chromosome in the GVBD and meiosis II (MII) stage oocytes (data not shown). Positive, diffuse staining was detected in the nucleus of GV stage, and at marginal

levels from the GVBD to M II stage. The distribution of H3K79me2 and H3K79me3 was consistent with Ooga's study (Ooga *et al.* 2008) (data not shown). The staining of H3K79me2 was detected in the whole genome at GV stage and all chromosomes after GVBD. The distribution of H3K79me3, however, was only presented in heterochromatin at DAPI-intense foci in nucleolus at GV stage and in chromosome after GVBD.

siRNA injection suppress the Dot1l expression and H3K79 methylation level effectively

To suppress *Dot1l* expression, the siRNA targeting *Dot1l* mRNA was injected into mouse GV oocytes as described previously (Wianny & Zernicka-Goetz 2000). After cultured in IVM medium with IBMX, the total RNA of oocytes was extracted for RT-qPCR. The results showed that the *Dot1l* mRNA was reduced to 32.8% ($p<0.01$) compared to no injection controls (Figure 1B). In contrast, there was no significant difference between the other treatments. The GV oocytes in each treatment were immunostained for checking the decreases in Dot1L protein and GVBD oocytes for H3K79 methylation. Because the H3K79me2 level was 30 folds than the H3K79me3 in mouse ES cells (Jones *et al.* 2008), we chose H3K79me2 level as a marker for evaluation of H3K79 methylation after siRNA injection. Accompanied the cleavage of *Dot1l* mRNA, Dot1L protein was reduced significantly as shown by immunocytochemistry 24 h after siRNA injection (Figure 1A,C). We also compared the Dot1L protein level in siRNA injection treatment and the scrambled RNA injection treatment by Western blotting (Figure 1D). The similar results were obtained. The results of Immunofluorescence analysis indicate that the H3K79me2 level after siRNA injection treatment was reduced dramatically than the other two treatments (Figure 2A,B). There was no significant difference between the scrambled RNA injection treatment and the no injection treatment.

Dot1L deficient oocytes show normal GVBD but low maturity ratio

The effects of Dot1L deficient on mouse oocytes meiosis were analyzed. First, the GVBD ratio was measured for each treatment after cultured in IVM medium for

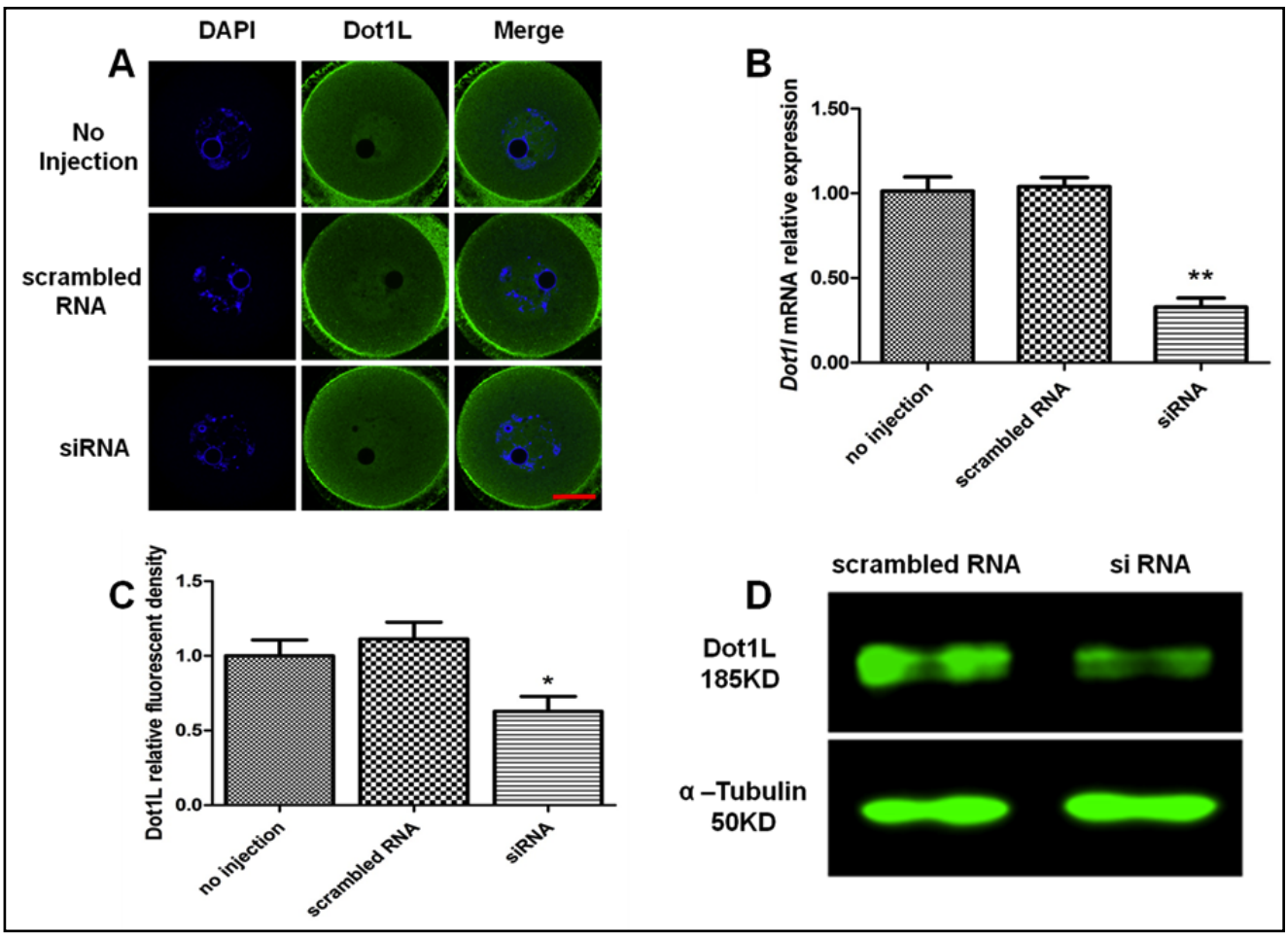

Fig. 1. siRNA injection suppresses the *dot1l* expression effectively. (A) Immunofluorescence staining by anti-Dot1L antibody in each treatment. Bar=25μm (B) The expression of *dot1l* was decreased after siRNA injected (** p<0.01). (C) Immunofluorescence staining semi-quantified data with Image J. Relative protein levels are presented as mean, standard deviation (s.d.) (* p<0.05). (D) Western blot analysis on Dot1L using extracts from GV oocytes of siRNA and scrambled RNA injected. α-tubulin as reference marker. Dot1L:185kDa, α-tubulin: 50 kDa.

2h. The results indicated that there was no difference between each two treatments, as shown by 88.9% (siRNA injection treatment: 232/261) versus 89.5% (scrambled RNA treatment: 221/247) and 91.1% (no injection treatment: 216/237) respectively (Figure 2C left, $p>0.05$). Then, we checked extrusion ratio of the first polar body (PB1%) after IVM cultured for 12h. Surprisingly, compared to scrambled RNA treatment and no injection treatment, the oocytes PB1% in the siRNA injection treatment was decreased dramatically, as shown by 44.8% (siRNA injection treatment: 117/261) versus 62.8% (scrambled RNA treatment: 155/247) and 61.6% (no injection treatment: 146/237) respectively (Figure 2C right, $p<0.01$).

There are two possibilities to explain the low maturity ratio of the Dot1L-deficient oocytes, i.e., the chromosome failed to condense or failed to divide. To understand the mechanism behind, the oocytes in each treatment were stained with DAPI. The results indicated that most of the oocytes with siRNA injected were blocked in metaphase of meiosis I. The immunofluorescence with an antibody against BubR1, a key protein involved in mouse mitosis and meiosis check-point, was applied. As expected, the results show that BubR1 remained on the chromosome in the oocytes with *Dot1l* siRNA injection after IVM 12h (Figure 2D), but almost disappeared in the other two treatments.

Dot1L deficient oocytes show deacetylated incompletely on the H3K27 and H4K12

Two meiotic acetylation markers, H3K27 acetylation (H3K27ac) and H4K12 acetylation (H4K12ac), were chosen for checking the acetylation on chromosomes in each treatment as previously described (Akiyama *et al.* 2006). Although there are similar patterns of H3K27ac and H4K12ac at GV oocytes in each treatment (data not shown), there are 57.7% (n=26) of the oocytes remained H3K27ac (Figure 3A) and 60.7% (n=28) of the oocytes remained H4K12ac (Figure 3B) in siRNA injection treatment, whereas only 18.5% (n=27) and 17.4% (n=23) remained the H3K27ac in scrambled RNA treatment and no injection treatment respectively (Figure 3A), only 13.8% (n=36) and 12.5% (n=32) remained the H4K12ac in scrambled RNA treatment

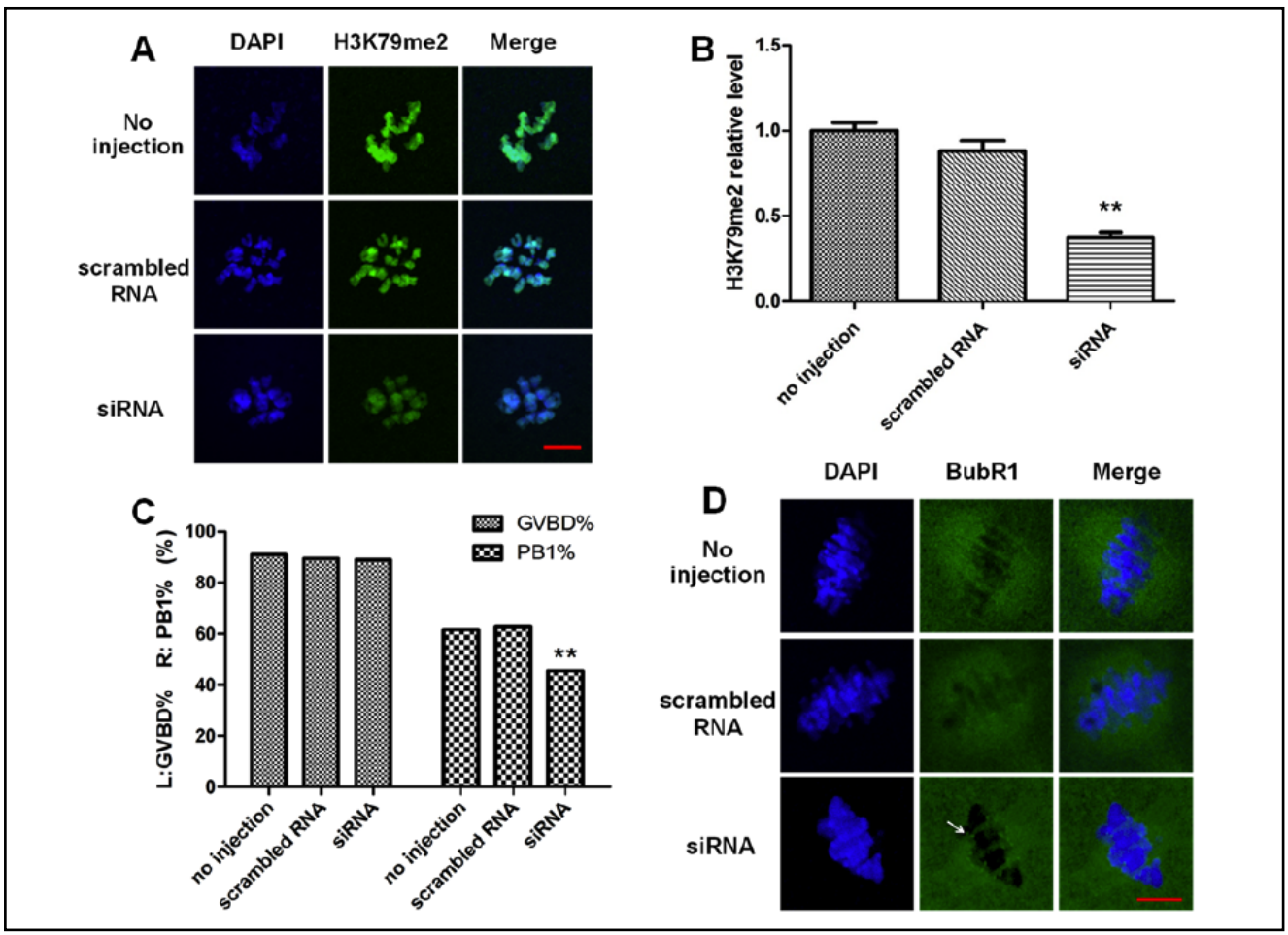

Fig. 2. siRNA injection suppresses H3K79me2 level, and result in low maturity ratio. (A) Immunofluorescence staining by anti-H3K79me2 antibody in each treatment. Bar=10μm. (B) Semi-quantified immunofluorescence data with Image J. Relative protein levels are presented as mean, standard deviation (s.d.) (** $p<0.01$). (C) Comparison of GVBD% and PB1% of each treatment. Oocytes number: siRNA: n=261, scrambled RNA: n=247, no injection: n=237 (X^2 test, ** $p<0.01$). (D)Immunofluorescence staining by anti-BubR1 antibody in each treatment. White arrow indicates BubR1 remains on the chromosome in siRNA injected oocytes. Bar=10μm.

and no injection treatment (Figure 3B). These results showed that histone was deacetylated incompletely in mouse oocytes with Dot1L deficiency.

DISCUSSION

There are three methylation states (mono-, di-, and tri-) on histone H3K79 in mouse genome and they are all catalyzed by a methyltransferase Dot1L. Monomethylation on H3K79 was usually considered to be a basic state (Jones *et al.* 2008). It has been reported that in human beings, methyltransferase domain of DOT1L can only di-methylate but not tri-methylate its substrate, and histone H2B ubiquitylated chemically stimulates hDOT1L mediated H3K79 trimethylation with the human DotCom (Mohan *et al.* 2010). We proposed that Dot1L probably was predominantly dissociative in GV oocyte and was part of large macromolecular complex after GVBD. It may be due to the same reason that there was only small fraction of spread nuclei from meiotic cells displaying Dot1 staining in yeast (San-Segundo & Roeder 2000). These results indicated that although Dot1L was the sole H3K79 methyltransferase in mouse oocytes, the H3K79me2 and H3K79me3 probably occurred under different mechanism.

In mouse, there are five alternative splicing variants (*Dot1l*a-*Dot1l*e) of *Dot1l* gene, and the Dot1L is the translation from the *Dot1la* (Zhang *et al.* 2004). The siRNA we designed to target *Dot1l* mRNA could recognize *Dot1l* variant a, b, and c. The level of *Dot1l* mRNA and Dot1L protein in mouse oocytes was down regulated effectively by injection of *Dot1l* siRNA.

Although Dot1-deficient *S. cerevisiae* showed normal cell numbers but defective spores (San-Segundo & Roeder 2000), our results indicates that the Dot1L deficient mouse GV oocytes could GV break down smoothly, but were blocked in metaphase of meiosis I. The Dot1-depended H3K79 methylation was involved in meiotic checkpoint control in yeast (San-Segundo & Roeder 2000), and both elevated apoptosis and G2 cell cycle arrest contributed to the reduced growth rate of *Dot1l* mutant mouse ES cells (Jones *et al.* 2008). Hence, we hypothesized that the checkpoint went wrong somehow in Dot1L deficient oocytes. It was confirmed subsequently by the immunocytochemistry results with an antibody against BubR1. In normal mitosis, the BubR1 was enriched at the microtubule-unattached kinetochore. When all the chromosomes were aligned at the spindle equator, the BubR1 was dephosphorylated and dropped from the kinetochore, then anaphase started (Jablonski *et al.* 1998). In Dot1L deficient oocytes, the BubR1 remained on the chromosome in metaphase of meiosis I.

In yeast, the *Δdot1* relieves the meiotic arrest of *Δzip1* (chromosomes fail to synapse) or *Δdmc1* (arrests in meiosis with unrepaired DSBs). The yeast strain of *zip1 dot1* double deletion or *dmc1 dot1* double deletion underwent high levels of meiotic nuclear division and sporulation, but viability of spore was decreased dramatically (San-Segundo & Roeder 2000). These results indicated that DOT1 is a key pachytene checkpoint protein in yeast. However, mouse GV oocytes were arrested in diplotene, at least one crossover between each pair of homologous chromosome. With *Dot1l* siRNA injected, the oocytes GVBD were accomplished smoothly, but for the BubR1 localization, a large part of oocytes was arrested at metaphase of meiosis I. Previous studies have shown that BubR1 was enriched at kinetochores unattached or attached improperly to the mitotic spindle during metaphase (Howell *et al.* 2004), and is reduced

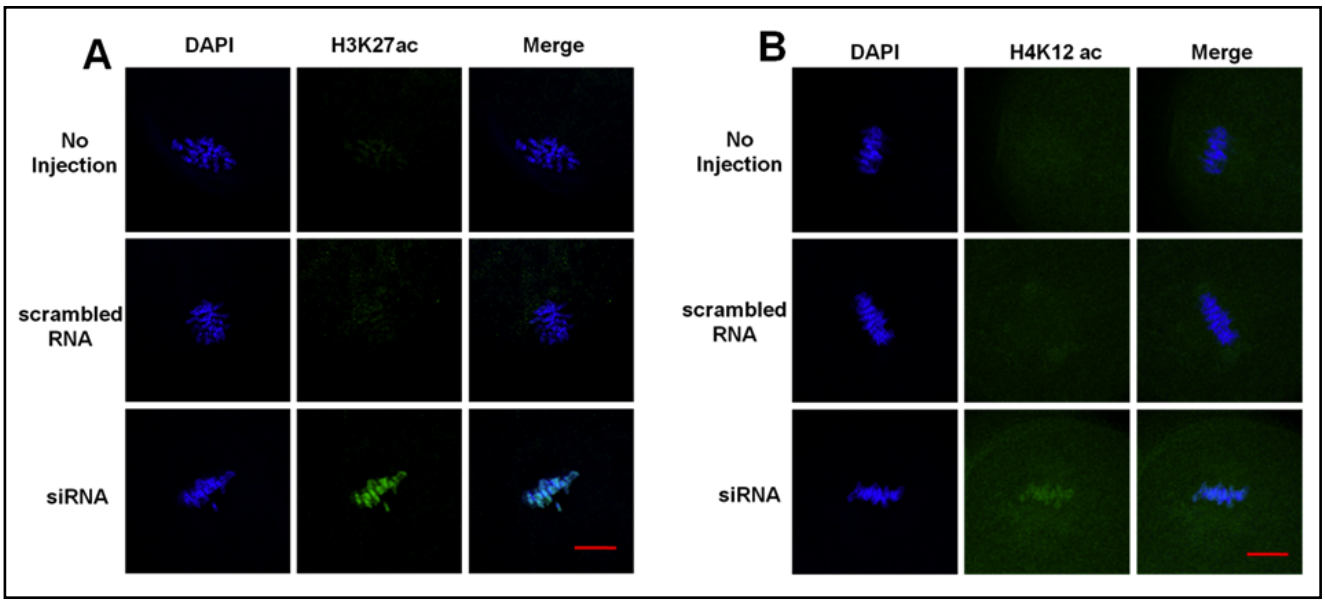

Fig. 3. Immunofluorescence staining by anti-H4K12ac antibody or anti-H3K27ac antibody in each treatment. Bar=20μm. (A) H4K12ac. (B) H3K27ac.

but not eliminated upon microtubule attachment in mitosis (Jablonski *et al.* 1998). It was also reported that mouse oocyte meiosis was arrested by over expression of BubR1 (Wei *et al.* 2010). These results indicated that the checkpoint of metaphase I to anaphase I worked efficiently after *Dot1l* siRNA injection and resulted in the oocyte meiotic arrest. BubR1 localizes to centrosomes (Tatum & Li 2011), H3K79me3 was also localized on centrosomes in mouse oocyte (Ooga *et al.* 2008), so we speculate that the H3K79me3 deficiency at the centrosomes maybe the key reason that the kinetochores-microtubule attachments could not be established properly.

DOT1 plays an important role in forming silent information regulator (SIR) complexes at telomeres. In strain of *dot1* mutant, the Sir2 and Sir3 proteins were dispersed to other locations of meiotic chromosome instead of in telomere in *S. cerevisiae* (San-Segundo & Roeder 2000). Sir2 can efficiently deacetylate histone (Grozinger *et al.* 2001), and over expression of Sir2 leads to global histone deacetylation (Braunstein *et al.* 1993). Thus, we predicted that deacetylation of histone maybe incomplete in Dot1L deficient mouse oocytes. It was confirmed subsequently by the immunocytochemistry results with an antibody against two meiotic acetylation markers, H3K27ac and H4K12ac.

Although level of heterochromatic marks (H3K9 di-methylation and H4K20 tri-methylation) at centromeres and telomeres were reduced in Dot1L deficient ES cells, the expression of their methyltransferases was at a normal level (Jones *et al.* 2008). This indicated that Dot1L deficiency may affect the targeting of H3K9 and H4K20 methyltransferases or demethylases to constitutive heterochromatin. Interestingly, in humans and *D. melanogaster*, the H3K9 methyltransferases could interact with histone deacetylase (HDAC), indicating the coupling of H3K9 methylation and histone deacetylation (Vaute *et al.* 2002). H3K79 tri-methylation also co-localized with HP1 in mouse oocytes, that suggesting an interaction between H3K79 tri-methylation and HP1 (Ooga *et al.* 2008). HDACs interact with HP1 as well (Zhang *et al.* 2002). These factors may cooperate to promote heterochromatin formation. Deacetylation of the histone tail facilitates H3K9 methylation, which in turn promotes HP1 binding and recruitment of additional HDACs and methyltransferases. Given the interactions between Sir2 and HP1, once initiated, such a complex could spread along the nucleosome array, and the H3 deacetylation was spread leading to heterochromatin (Vaute *et al.* 2002; Zhang *et al.* 2002). Histones of chromosome were deacetylated dramatically in mouse oocyte after GVBD (Kim *et al.* 2003). The acetylation of H3K27 and H4K12 was deacetylated incompletely in RNAi oocytes, suggesting that H3K79 methylation acts upstream of histone deacetylation and may play an important role in histone deacetylation in mouse oocytes.

CONCLUSIONS

We have provided for the first evidence that Dot1L is localized in subnuclear of mouse oocytes. The Dot1l expression and H3K79 methylation level could be suppressed effectively by using siRNA injection method. Our results prove that the meiosis I, accompany with BubR1 remaining on the chromosome, was interrupted in metaphase in Dot1L deficient mouse oocytes. This indicates that Dot1L and H3K79 methylation are critical to the metaphase-anaphase checkpoint. Our findings indicate that histone was deacetylated incompletely in mouse oocytes with Dot1L deficiency. Hence, taken together, Dot1L mediated H3K79 methylation is essential for first meiosis during meiotic maturation in mouse oocytes.

ACKNOWLEDGEMENT

This work was supported by grants from National Natural Science Foundation of China (30771552) and National Basic Research Program of China (2007CB947403).

REFERENCE

1 Akiyama T, Nagata M, Aoki F (2006). Inadequate histone deacetylation during oocyte meiosis causes aneuploidy and embryo death in mice. Proc Natl Acad Sci U S A **103**: 7339–7344.
2 Barski A, Cuddapah S, Cui K, Roh TY, Schones DE, Wang Z, Wei G, Chepelev I, *et al.* (2007). High-resolution profiling of histone methylations in the human genome. Cell **129**: 823–837.
3 Braunstein M, Rose A, Holmes S, Allis C, Broach J (1993). Transcriptional silencing in yeast is associated with reduced nucleosome acetylation. Genes & Development **7**: 592–604.
4 Feng Q, Wang H, Ng HH, Erdjument-Bromage H, Tempst P, Struhl K, Zhang Y (2002). Methylation of H3-lysine 79 is mediated by a new family of HMTases without a SET domain. Curr Biol **12**: 1052–1058.
5 Grozinger CM, Chao ED, Blackwell HE, Moazed D, Schreiber SL (2001). Identification of a class of small molecule inhibitors of the sirtuin family of NAD-dependent deacetylases by phenotypic screening. Journal of Biological Chemistry **276**: 38837–38843.
6 Hara KT, Sakuma Y, Sakai S, Nagata M, Aoki F (2003). Dynamic changes in the expression of protein tyrosine phosphatases during preimplantation mouse development: semi-quantification by real-time PCR. J Reprod Dev **49**: 323–328.
7 Howell BJ, Moree B, Farrar EM, Stewart S, Fang G, Salmon ED (2004). Spindle checkpoint protein dynamics at kinetochores in living cells. Curr Biol **14**: 953–964.
8 Jablonski SA, Chan GK, Cooke CA, Earnshaw WC, Yen TJ (1998). The hBUB1 and hBUBR1 kinases sequentially assemble onto kinetochores during prophase with hBUBR1 concentrating at the kinetochore plates in mitosis. Chromosoma **107**: 386–396.
9 Jones B, Su H, Bhat A, Lei H, Bajko J, Hevi S, Baltus GA, Kadam S, *et al.* (2008). The histone H3K79 methyltransferase Dot1L is essential for mammalian development and heterochromatin structure. PLoS Genet **4**: e1000190.
10 Kim JM, Liu H, Tazaki M, Nagata M, Aoki F (2003). Changes in histone acetylation during mouse oocyte meiosis. J Cell Biol **162**: 37–46.

11 Kim S-K, Jung I, Lee H, Kang K, Kim M, Jeong K, Kwon CS, Han Y-M, *et al.* (2012a). Human Histone H3K79 Methyltransferase DOT1L Methyltransferase Binds Actively Transcribing RNA Polymerase II to Regulate Gene Expression. Journal of Biological Chemistry **287**: 39698–39709.
12 Kim W, Kim R, Park G, Park J-W, Kim J-E (2012b). Deficiency of H3K79 histone methyltransferase Dot1-like protein (DOT1L) inhibits cell proliferation. Journal of Biological Chemistry **287**: 5588–5599.
13 Kouzarides T (2007). Chromatin modifications and their function. Cell **128**: 693–705.
14 Li B, Carey M, Workman JL (2007). The role of chromatin during transcription. Cell **128**: 707–719.
15 Liu H, Kim JM, Aoki F (2004). Regulation of histone H3 lysine 9 methylation in oocytes and early pre-implantation embryos. Development **131**: 2269–2280.
16 Mohan M, Herz HM, Takahashi YH, Lin C, Lai KC, Zhang Y, Washburn MP, Florens L, *et al.* (2010). Linking H3K79 trimethylation to Wnt signaling through a novel Dot1-containing complex (DotCom). Genes Dev **24**: 574–589.
17 Oksenych V, Zhovmer A, Ziani S, Mari P-O, Eberova J, Nardo T, Stefanini M, Giglia-Mari G, *et al.* (2013). Histone Methyltransferase DOT1L Drives Recovery of Gene Expression after a Genotoxic Attack. PLoS genetics **9**: e1003611.
18 Ontoso D, Kauppi L, Keeney S, San-Segundo PA (2013). Dynamics of DOT1L localization and H3K79 methylation during meiotic prophase I in mouse spermatocytes. Chromosoma: 1–18.
19 Ooga M, Inoue A, Kageyama S, Akiyama T, Nagata M, Aoki F (2008). Changes in H3K79 methylation during preimplantation development in mice. Biol Reprod **78**: 413–424.
20 Peters AH, O'carroll D, Scherthan H, Mechtler K, Sauer S, Schofer C, Weipoltshammer K, Pagani M, *et al.* (2001). Loss of the Suv39h histone methyltransferases impairs mammalian heterochromatin and genome stability. Cell **107**: 323–337.
21 Pokholok DK, Harbison CT, Levine S, Cole M, Hannett NM, Lee TI, Bell GW, Walker K, *et al.* (2005). Genome-wide map of nucleosome acetylation and methylation in yeast. Cell **122**: 517–527.
22 San-Segundo PA, Roeder GS (2000). Role for the silencing protein Dot1 in meiotic checkpoint control. Mol Biol Cell **11**: 3601–3615.
23 Singer MS, Kahana A, Wolf AJ, Meisinger LL, Peterson SE, Goggin C, Mahowald M, Gottschling DE (1998). Identification of high-copy disruptors of telomeric silencing in Saccharomyces cerevisiae. Genetics **150**: 613–632.
24 Tatum D, Li S (2011). Evidence that the histone methyltransferase Dot1 mediates global genomic repair by methylating histone H3 on lysine 79. J Biol Chem **286**: 17530–17535.
25 Vaute O, Nicolas E, Vandel L, Trouche D (2002). Functional and physical interaction between the histone methyl transferase Suv39H1 and histone deacetylases. Nucleic Acids Res **30**: 475–481.
26 Wei L, Liang XW, Zhang QH, Li M, Yuan J, Li S, Sun SC, Ouyang YC, *et al.* (2010). BubR1 is a spindle assembly checkpoint protein regulating meiotic cell cycle progression of mouse oocyte. Cell Cycle **9**.
27 Wianny F, Zernicka-Goetz M (2000). Specific interference with gene function by double-stranded RNA in early mouse development. Nat Cell Biol **2**: 70–75.
28 Yu J, Deng M, Medvedev S, Yang J, Hecht NB, Schultz RM (2004). Transgenic RNAi-mediated reduction of MSY2 in mouse oocytes results in reduced fertility. Dev Biol **268**: 195–206.
29 Zhang CL, Mckinsey TA, Olson EN (2002). Association of class II histone deacetylases with heterochromatin protein 1: potential role for histone methylation in control of muscle differentiation. Mol Cell Biol **22**: 7302–7312.
30 Zhang W, Hayashizaki Y, Kone BC (2004). Structure and regulation of the mDot1 gene, a mouse histone H3 methyltransferase. Biochem J **377**: 641–651.